

RESOLUTION OF THREE-DIMENSIONAL MT INVERSION FOR GEOTHERMAL EXPLORATION

Toshihiro Uchida

Geological Survey of Japan, AIST, Tsukuba 305-8567, Japan

ABSTRACT

Dependency of three-dimensional (3-D) inversion of magnetotelluric (MT) data on the observation error and the station interval was examined. The 3-D inversion technique, which was used in this work, utilizes the finite difference method for the forward modeling and the least-squares method for the inversion part. The inversion incorporates the observation error as the weight in the Jacobian matrix. Experiments with the MT data obtained in the Northern Negros geothermal field, central Philippines, with different weight settings indicated that an accurate estimate of the observation error in the field measurement and an appropriate setting of the weights for the Jacobian matrix in the inversion are important to obtain reliable 3-D models.

The interval of MT stations is a difficult decision in the field design. The effect of the station interval on 3-D inverted models was examined using a large volume MT dataset obtained in the Ogiri geothermal area, Japan. The average station interval of the Ogiri MT survey was approximately 250 m. 3-D inversions were conducted using several subsets of the data. When the station interval is around 1 km, the resultant 3-D model is lacking a resolution for delineating the reservoir structure. This suggests that the station interval should be less than several hundreds meters, when we seek for detailed imaging of geothermal reservoirs at a depth range of 500 – 2000 m.

1.0 INTRODUCTION

The MT method is one of the essential tools for investigating geological structure in geothermal exploration. It is mainly because of its capability to delineate low-resistivity anomalies associated with the reservoir structure. Experiences of 2-D inversion of MT data in geothermal fields by many geophysicists in the past decade have

revealed the effectiveness of the MT method in investigating geothermal reservoirs. In addition, it has been recognized that sophisticated 3-D interpretation techniques are also demanded for precise delineation of reservoir structure in a complex geologic environment. Although the 3-D interpretation of MT data is still very costly and time consuming, it has become practical in these few years owing to newly developed inversion techniques (e.g., Sasaki, 1999; Zhdanov *et al.*, 2000; Mackie *et al.*, 2001).

Sasaki (1999) developed a 3-D MT inversion technique and tested it with several synthetic datasets. Sasaki (2001) proposed to estimate static shifts simultaneously by the inversion. Uchida *et al.* (2002) and Uchida and Sasaki (2003) applied the method to the MT data obtained in geothermal fields in Indonesia and Japan, showing that the 3-D inversion code can be applied to almost any field dataset that has an irregular station arrangement or is contaminated by artificial and natural noises.

In this paper, I examined effects of the station interval of the MT stations on the final 3-D models. It is to provide an appropriate guideline on the site arrangement of an MT survey for geothermal exploration, because the site design is very crucial at the beginning of an MT survey. I also tested the effects of the weight setting when we construct a Jacobian matrix in the inversion. Since the observation errors obtained in the field measurements are often ambiguous, we need to set the weight for each data adequately.

2.0 INVERSION METHOD

The 3-D inversion scheme used in this work is based on the linearized iterative least-squares method with smoothness regularization (Sasaki, 1999). The forward modeling for a given arbitrary 3-D earth is by the finite difference method. For a finite difference with a staggered

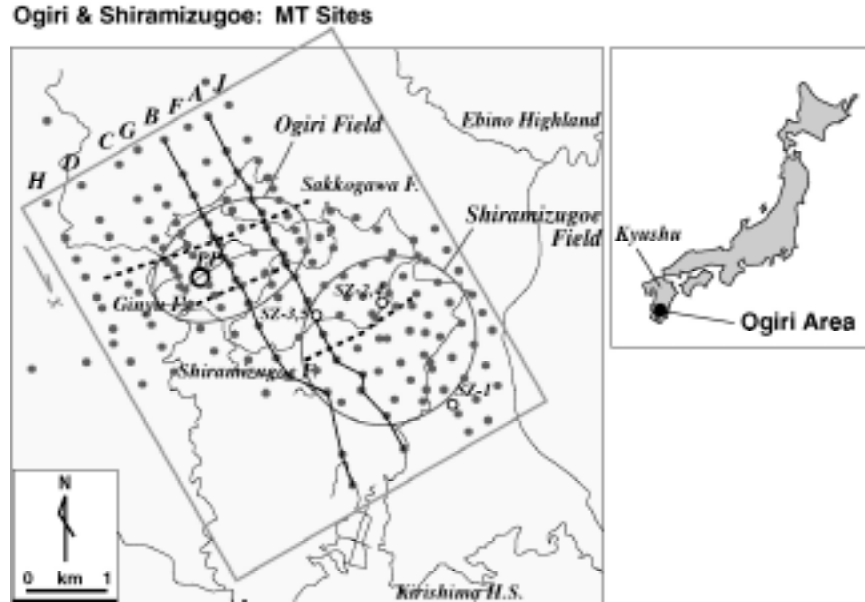


Figure 1. MT stations over the Ogiri and Shiramizugoe geothermal fields, southwestern Japan. Dots are MT stations, small open circles are pilot drillings, the large open circle with the letters PP is the Ogiri power plant, large ovals indicate centers of two geothermal fields, dashed lines are estimated faults, and thin solid lines are local roads. Letters A-H indicate names of the NW-SE survey lines. Lines A and B are shown with thick solid lines. The large inclined rectangle indicates the region of 3-D interpretation.

grid, the solution region, including both air and earth, is discretized into rectangular cells. The topography is not incorporated. In addition to block resistivities of a 3-D model, static shifts are also treated as unknowns in the inversion (Sasaki, 2001).

The objective function U to be minimized in the inversion is defined as,

$$U = \|\mathbf{W}[\mathbf{d} - F(\mathbf{m}) - \mathbf{G}\mathbf{s}]\|^2 + \alpha^2 (\|\mathbf{C}\mathbf{m}\|^2 + \beta^2 \|\mathbf{s}\|^2) \quad (1)$$

where \mathbf{W} is the weight defined from observation errors, \mathbf{d} is the observed data (apparent resistivity and phase), \mathbf{m} is a 3-D resistivity model, F is a non-linear function that works on the model \mathbf{m} to produce MT responses, \mathbf{C} is a roughening matrix, \mathbf{s} is the static shift, and \mathbf{G} is a matrix that relates static shifts and the MT responses. The first term of the right-hand side is for the misfit minimization and the second term is for roughness and static-shift minimization. The α and β are trade-off parameters for roughness minimization and static-shift minimization, respectively, with regard to the misfit minimization.

3.0 STATION INTERVAL

The station interval is an important factor for the survey design. I applied the 3-D inversion to a large volume MT field dataset obtained in the Ogiri geothermal area, southwestern Japan, in order to examine the effect of the station interval on the final resistivity model.

The Ogiri geothermal area is located in a southern part of Kyushu Island (Fig. 1). A 30-MWe geothermal power plant has been in operation by Nittetsu Kagoshima Geothermal Co., Ltd. (NKG) since 1996. The Shiramizugoe field, neighboring to the Ogiri field, is estimated to be a promising field for future exploitation. The survey area is situated on a highland whose elevation is from 700 m to 900 m. The area is underlain by Quaternary volcanic rocks with a thickness of more than 2 km. Below this layer is a Mesozoic metamorphic formation that forms the basement layer of this region. Three faults in an ENE-WSW direction have been identified in the survey area: Sakkogawa, Ginyu and Shiramizugoe from north to south. The major production zone of the Ogiri geothermal reservoir is associated with the Ginyu Fault (Goko, 2000). A new geothermal resource is under exploration by targeting the Shiramizugoe

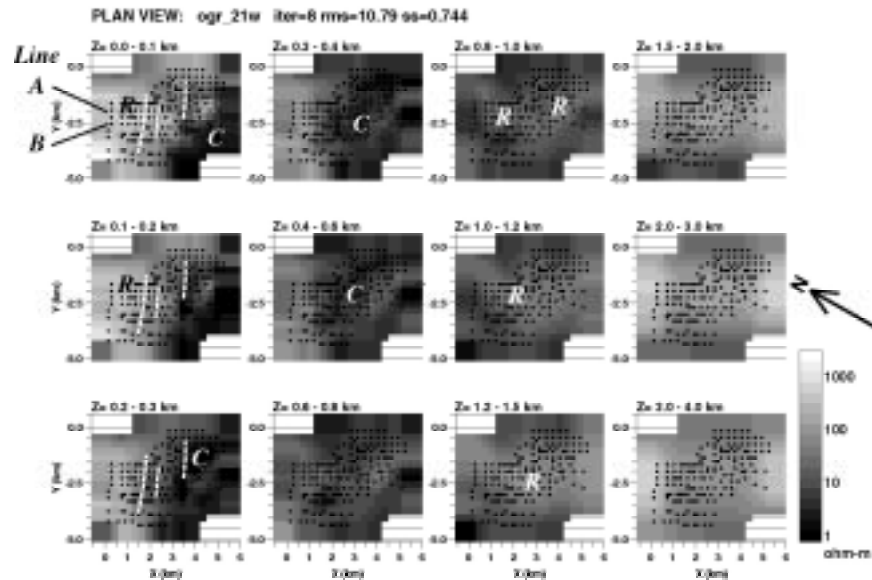


Figure 2. Depth-slice resistivity sections of a 3-D model of the Ogiri MT data using all sites. Upper-left panel shows the shallowest section, and lower and right panels are deeper sections. Black dots indicate the MT sites. The x-direction is 150 degrees clockwise from north. Letters C and R indicate typical conductive and resistive anomalies, respectively. White dashed lines on the left panels are estimated faults, and Letters A and B indicate two survey lines.

Fault. The geothermal reservoir in this area is distributed in the Quaternary volcanic layers that are mostly consisting of tuff and lava erupted from young volcanoes to the south and east of the area. The heat source of the current reservoir system is estimated to be an active volcano, a few kilometers to the east of the survey area. The MT data in this area were obtained by the New Energy and Industrial Technology Development Organization (NEDO), NKG, and Geological Survey of Japan (GSJ) at several stages since 1996. Intensive surveys were conducted by NEDO at Ogiri in 1999 for precise reservoir monitoring and at Shiramizugoe in 2000 for exploration of a new geothermal field. Several survey lines were set in the NW-SE direction so that they were perpendicular to the geologic strike, which is the direction of the faults.

The total number of MT stations used for the 3-D inversion is 158 (Fig. 1). For the 3-D inversion, the MT impedance was rotated to a direction of 60 degrees clockwise from north. Directions of x- and y-axes are 150 and 60 degrees, respectively. The number of frequencies used for the inversion is 11 (from 0.0703 Hz to 72 Hz). The average station interval is 230 m. First, I used all stations for the inversion (Whole-set); then, re-sampled the stations and made two

subsets of the data. The number of the stations is 46 for Subset-1 and 18 for Subset-2. The average station intervals of these datasets are 540 m for Subset-1 and 900 m for Subset-2.

Figure 2 shows depth-slice sections by the inversion of the Whole-set data. The normalized RMS misfit, assuming a noise floor of 1% (see later section), is 10.79, and the average of the estimated static shifts is 0.744 in the natural logarithmic domain. Resistivity structure of this area is characterized by a three-layer model: resistive first layer, conductive second layer and resistive third layer. Resistivity distribution of the shallow layers (less than a depth of 300 m) has a clear contrast between the high-resistivity zone in the northern half of the survey area and the low-resistivity zone in the southern half. At the mid depth, say from 400 m to 800 m, the whole area shows low resistivity. Then below a depth of about 800 m, high-resistivity anomalies are recognized at the center of the area, and they occupy the whole area at a depth of 2 km.

Figures 3 and 4 compare the inversion of three datasets: Whole-set, Subset-1 and Subset-2. Figure 3 shows three depth-sections and Figure 4 shows two vertical sections along Lines A and B. The number of the resistivity blocks, whose resistivity values are unknown in

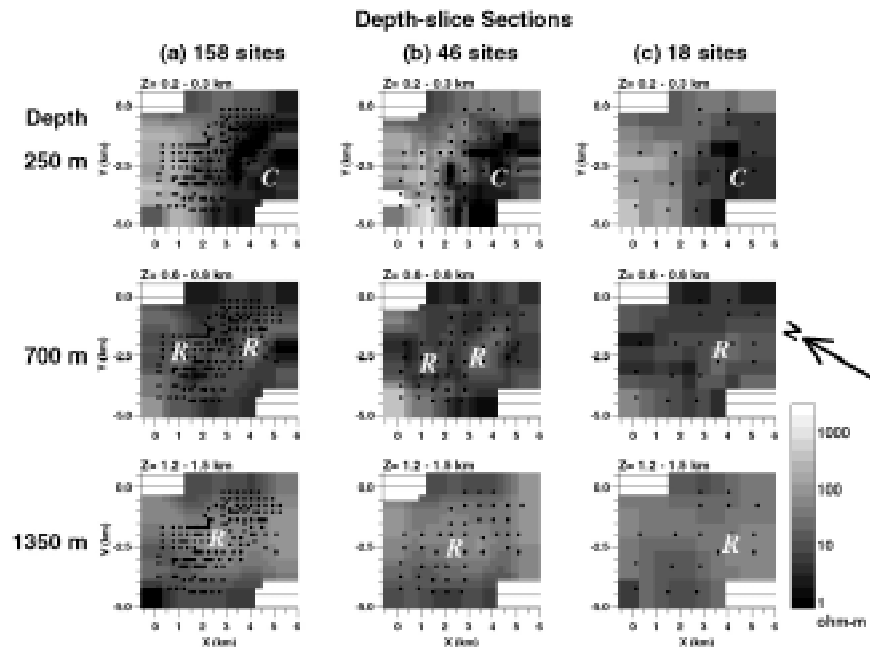


Figure 3. Depth-slice resistivity sections of the 3-D models at three depths with different number of MT sites: (a) 158 sites, (b) 46 sites and (c) 18 sites. Black dots indicate the MT sites. Letters C and R indicate typical conductive and resistive anomalies, respectively.

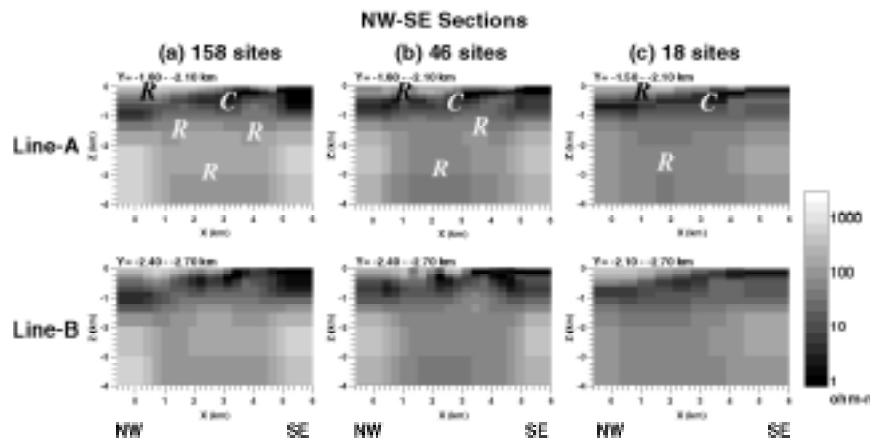


Figure 4. Vertical sections from the 3-D models along Lines A and B for three different number of MT sites: (a) 158 sites, (b) 46 sites and (c) 18 sites.

the inversion, is 3780 for the Whole-set and Subset-1, while that of Subset-2 is 1008. The horizontal size of the blocks is 300 m for the first two cases (Whole-set and Subset-1) and 600 m for Subset-2. At a depth of 250 m, the Whole-set and Subset-1 were able to delineate low resistivity anomalies associated with the faults (Ginyu and Shiramizugoe Faults). However, Subset-2 lost a resolution and was unable to detect them (Fig. 3). At a depth of 700 m, the first two sets detected two high-resistivity anomalies in the center of the section, while

Subset-2 only detected the resistive anomaly in the right-hand side. Shapes of high-resistivity zones in the center at a depth of 1350 m are similar between the Whole-set and Subset-1.

Comparison of the vertical sections along Lines A and B indicated that the boundary between the resistive first layer and the conductive second layer is almost similar among three models (Fig. 4). However, the boundary between the conductive second layer and the resistive third layer differs among them. For the

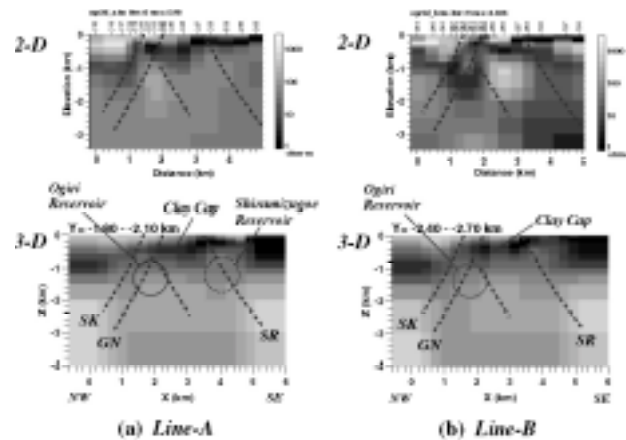


Figure 5. Comparison of 2-D and 3-D models along (a) Line-A and (b) Line-B. The 2-D models (upper panels) are from the inversion of TM-mode MT data. The lower panels are vertical sections from the 3-D model shown in Figure 2. Thick dashed lines are estimated faults. Large circles are estimated location of the production zones.

Whole-set model, the resistive third layer becomes shallow at two locations; x-distance is about 1.5 km and 4 km on both lines. On the other hand, the anomaly at $x = 1.5$ km is slightly unclear for Subset-1, and both anomalies are not clear for Subset-2.

Figure 5 shows a simple geologic interpretation as well as a comparison between 2-D and 3-D inversion models on Lines A and B. The low-resistivity second layer represents a zone of intensive clay alteration layer, where low-temperature clay minerals such as smectite were identified from drilling cores and cuttings. The production zone for the Ogiri power plant coincides on the shallow anomaly of the resistive third layer at $x = 1.5$ km on both lines. The Shiramizugoe reservoir identified by several exploration wells is located at another shallow anomaly at $x = 4$ km. This agreement suggests that the vertical sections by the Whole-set inversion is more reliable for the interpretation of the reservoir model. Therefore, the station interval should be smaller than several hundreds meters for the investigation of geothermal reservoir at a depth of 0.5 to 2 km, like the case of the Ogiri area.

4.0 NOISE FLOOR

To solve the inversion equation described by Equation (1), we assign a weight to each data to construct the matrix \mathbf{W} . The weight is usually a reciprocal of an observation error (standard deviation). If the observation errors are correctly

estimated from the field measurement and follow a Gaussian distribution, it is better to use them directly for the weights. However, the observation errors are often poorly estimated and the data are biased. We therefore usually set what we call a “noise floor.” If an estimated error is smaller than a preset level, which is a noise floor, we assume that the observation error of the data is the value of the noise floor. It prevents us to assign a too large weight to a data that has a very small observation error but is biased by an unknown coherent.

I examined the effect of the noise floor on 3-D inversion results with the MT data obtained in the Northern Negros Geothermal field (NNGF), central Philippines, by PNOC Energy Development Corporation (Maneja *et al.*, 2001). The data acquisition was done without the remote reference analysis. Therefore some parts of the data might be contaminated by local noises, even though overall data quality seems to be fine when we examine the MT sounding curves.

Figure 6 shows the MT stations in the NNGF. The survey area is located on the northwestern flank of the Canlaon Volcano, Negros Island, which is an active volcano. This area is mostly underlain by Quaternary volcanic rocks that overlie Tertiary sedimentary formations. There are numerous surface manifestations, including hot springs at Saray, Pataan, Hagdan and Mambucal. PNOC-EDC drilled several exploration wells in this area, and found promising geothermal resources beneath the

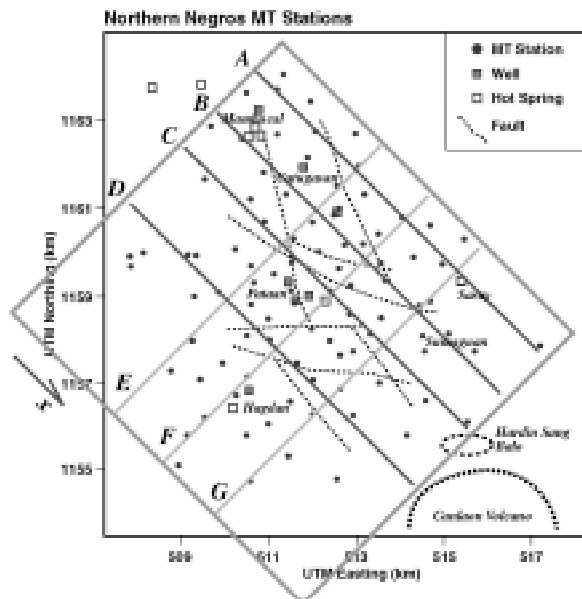


Figure 6. Location of MT stations (dots) in the Northern Negros geothermal field. Thin dashed lines are estimated faults, open squares are hot springs, solid squares are geothermal wells, and thick dashed lines indicate volcano summit or crater rim. Large inclined rectangle indicates the region for 3-D interpretation, and grey lines with letters A – G are hypothetical lines for interpretation of the 3-D model.

Pataan sector (Maneja *et al.*, 2001). For the 3-D inversion, the MT impedance was rotated to the direction of 45 degrees clockwise from north. Directions of x- and y-axes are 135 and 45 degrees, respectively. The number of MT

stations and frequencies used for the inversion are 92 and 11 (from 0.0703 Hz to 72 Hz), respectively. The average station interval is 570 m. Total number of the observed data is 3942; the number of the resistivity blocks is 2912.

Uchida *et al.* (2003) presented a preliminary 3-D inversion result by setting a noise floor of 1% in apparent resistivity. I then continued more trials of inversion by using different noise floors. Figure 7 compares vertical sections along four NW-SE lines (A, B, C and D) with three different noise floors: 1%, 3% and 5%. The model with the 1% noise floor has spurious anomalies at shallow parts of the sections, particularly on Lines A and B. Models by 3% and 5% noise floors show smoother resistivity distribution. These two models are almost similar. The roughness of the resistivity distribution (L-2 norm of **Cm** in Equation (1)) is 675, 187 and 198 for the models by 1%, 3% and 5% noise floors, respectively. This indicates that the model of 1% noise-floor is suffering from ambiguous resistivity parameters. It may be because resistivities of the model were improperly interpreted by biased apparent resistivity data that have small observation errors less than 3%. For another comparison, I conducted more experiments of the noise floor with the Ogiri MT data and those from the Central Leyte geothermal field (Rigor *et al.*, pers. comm.). However, they did not show large difference in the final 3-D models when the noise floor was changed from 1% to 3%. If the noise estimate of

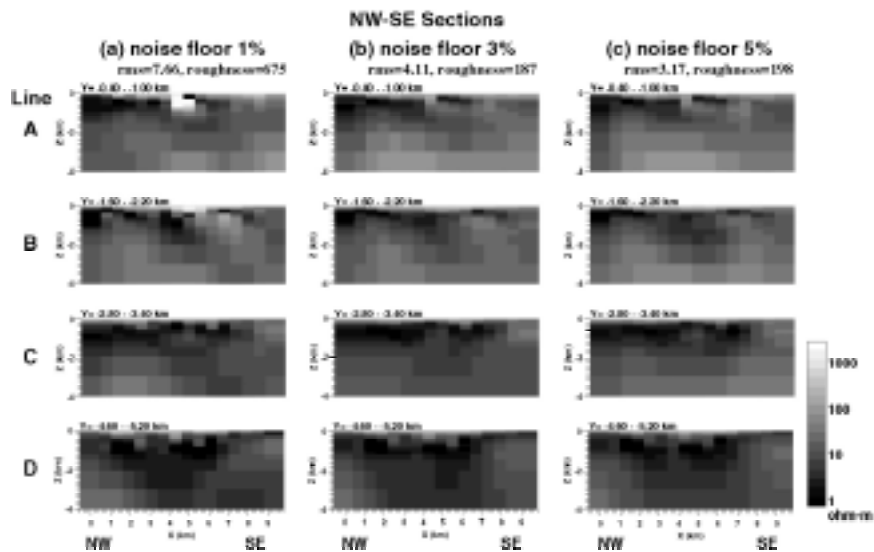


Figure 7. NW-SE vertical sections of the 3-D model of the Northern Negros MT data along four lines A - D with three different noise-floor settings: (a) 1%, (b) 3% and (c) 5%.

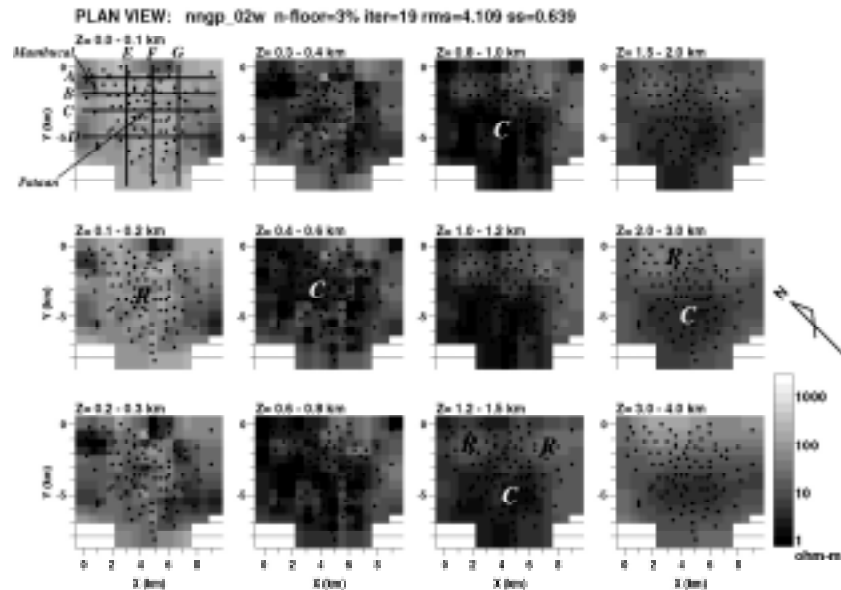


Figure 8. Depth-slice resistivity sections of the 3-D model of the Northern Negros MT data by the 3% noise-floor inversion. Upper-left panel shows the shallowest section, and lower and right panels are deeper sections. Black dots indicate the MT sites. The x-direction is 135 degrees clockwise from north. Black lines on the upper-left panel indicate hypothetical lines for further interpretation.

observed data is appropriate, the effect of the noise-floor setting does not seem to be so significant.

I have chosen the model by 3% noise-floor for further interpretation of the NNGF MT data, because it has the smallest roughness among them. Figure 8 shows depth-slice sections of the 3-D model by the 3% noise-floor inversion. This area generally has a three-layer earth from a point of resistivity structure. The shallow layer, down to a 200 m depth, is generally of high resistivity over the entire area. The low-resistivity second layer is very thick, depths from 400 m to 1,000 m in average, and it continues to deep in the southwestern half of the survey area. The third layer is resistive and its top boundary is at a depth of about 1,000 m in the northeastern half of the area.

Figure 9 shows three vertical sections along NW-SE and SW-NE directions. Line C in the NW-SE direction intersects Lines E and F near the drilling sites at the Pataan sector. The conductive second layer is thicker in the west of the Pataan sector, while the resistive third layer becomes shallow in the east of the sector. The successful wells in the sector were drilled with a deviation toward the east (Maneja *et al.*, 2001). The sector is located at the boundary of the thick

conductive second layer in the west and the shallow resistive third layer in the east.

5.0 CONCLUSIONS

An appropriate station interval has been examined by using a large volume MT dataset obtained in the Ogiri geothermal area. Tests with several re-sampled small-volume datasets have suggested that the station interval should be less than several hundred meters when we seek for a resistivity structure at a depth range of 500 m – 2000 m, which is typical for a geothermal reservoir. If the station interval is about 1 km or larger, we would lose a resolution of the targeted structure in a 3-D inverted model.

An appropriate estimate of observation errors is found to be very important in the weighted least-squares inversion. Improper setting of the noise floor may result in an inappropriate 3-D model if the observed data contain biased errors. In the case of the MT data in the Northern Negros geothermal field, a noise floor of 3% or 5% in apparent resistivity was appropriate to avoid spurious anomalies that might be caused by biased noises. It is of course more important to avoid noises in the field measurement and to estimate the observation errors properly.

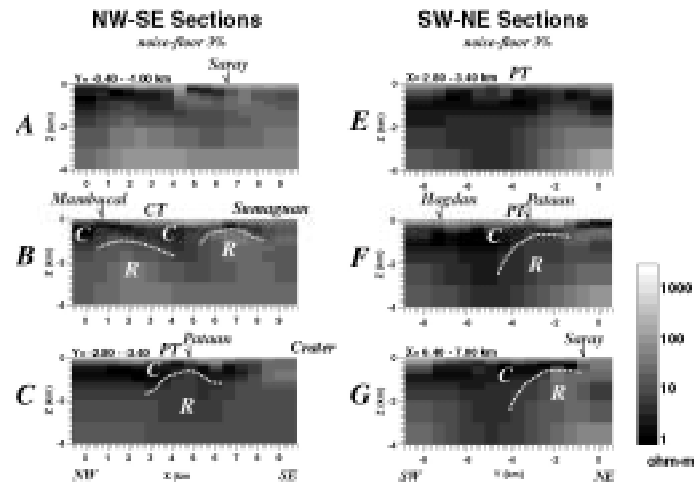


Figure 9. Vertical sections from the 3-D model of the Northern Negros MT data by 3% noise-floor inversion. Location of Lines A - G are shown in Figure 8. Locality names with arrows indicate hot spring, and letters PT and CT are projected location of drilling sites.

ACKNOWLEDGMENTS

The author thanks PNOC-EDC, NEDO and NKG for providing the MT field data in the Northern Negros geothermal field and Ogiri area for this research.

REFERENCES

- Goko, K. (2000). Structure and hydrology of the Ogiri field, West Kirishima geothermal area, Kyushu, Japan: *Geothermics*, 29, 127-149.
- Mackie, R., Rodi, W., and Watts, M. D. (2001). 3-D magnetotelluric inversion for resource exploration: Expanded Abstracts. Society of Exploration Geophysicists 71st Annual Meeting, 1501-1504.
- Maneja, F.C., Los Baños, C.F., Layugan, D.B., Apuada, N.A., and Rigor, D.M. Jr. (2001). Magnetotelluric sounding in the Northern Negros geothermal field, Central Philippines. *Journal of Geological Society of the Philippines*, 56, 184-198.
- Sasaki, Y. (1999). 3-D inversion of electrical and electromagnetic data on PC. Proceedings, 2nd International Symposium on Three-Dimensional Electromagnetics, 128-131.
- Sasaki, Y. (2001). Three-dimensional inversion of static-shifted magnetotelluric data. Proceedings, 5th SEGJ International Symposium, 185-190.
- Uchida, T., Lee, T.J., Honda, M., Ashari, and Andan, A. (2002). 2-D and 3-D interpretation of magnetotelluric data in the Bajawa geothermal field, central Flores, Indonesia. *Bulletin of Geological Survey of Japan*, 53, 265-283.
- Uchida, T., Layugan, D.B., Rigor Jr., D.M., Los Baños, C. F., Apuada, N.A., Olivar R.E.R., and Catane, J.P.L. (2003). 3-D interpretation of magnetotelluric data in Central Leyte and Northern Negros geothermal areas, central Philippines. Proceedings, 24th Annual PNOC-EDC Geothermal Conference, 73-78.
- Uchida, T. and Sasaki, Y. (2003). Stable 3-D inversion of MT data and its application to geothermal exploration: in Macnae, J. and Liu, G. (eds.), *Three-Dimensional Electromagnetics III*, ASEG, 12, 1-10.
- Zhdanov M.S., Fang, S., and Hursin, G. (2000). Electromagnetic inversion using quasi-linear approximation. *Geophysics*, 65, 1501-1513.